

JCTC

Journal of Chemical Theory and Computation

A Fast QM/MM (Quantum Mechanical/Molecular Mechanical) Approach to Calculate Nuclear Magnetic Resonance Chemical Shifts for Macromolecules

Bing Wang and Kenneth M. Merz, Jr.^{*,†}

104 Chemistry Building, The Pennsylvania State University,
University Park, Pennsylvania 16802

Received August 23, 2005

Abstract: A fast approach to calculate nuclear magnetic resonance (NMR) chemical shifts within the quantum mechanical/molecular mechanical (QM/MM) framework has been developed. The QM treatment is based on our recently implemented MNDO/NMR method (Wang et al. *J. Chem. Phys.* **2004**, 120, 11392). The effect of the QM/MM partitioning on chemical shifts has been investigated by test calculations on the water dimer and on the protein crambin. It has been shown that the quantum mechanical treatment of the hydrogen bond and nearby groups with significant magnetic susceptibilities is necessary in order to reproduce the full QM results. The method is also applied to a protein–ligand complex FKBP-GPI, and excellent agreement for proton chemical shifts of the ligand is obtained by including the side-chain atoms of the binding site residues into the QM region. The NMR chemical shift calculations using QM/MM-minimized structures still yield satisfactory results. Our results demonstrate that this QM/MM NMR method is able to treat critical regions of very large macromolecules without compromising accuracy if a relatively large QM region is used.

I. Introduction

Over the past several decades, nuclear magnetic resonance (NMR) spectroscopy has emerged as a powerful tool to study the structure and dynamics of biological systems.¹ One of its essential parameters is the NMR chemical shift that characterizes the chemical environment of individual atoms. Although it has been shown that the NMR chemical shift can provide useful information for protein secondary structures,² its complicated relationship with molecular structures hinders its application in protein structure determination and other NMR studies of biological systems. NMR chemical shifts are sensitive to subtle changes in electronic structure from local variations in bond lengths and bond and torsional angles, to electrostatic interactions, to hydrogen bonds, and

to magnetic susceptibility effects. In principle, the quantum mechanical theory of chemical shieldings is able to capture all of these contributions and predict chemical shifts accurately. Indeed, it has been demonstrated that calculated ¹H and ¹³C chemical shifts using reasonable basis sets at the Hartree–Fock and density functional theory (DFT) levels can predict experimental values for a variety of organic molecules with excellent accuracy.^{3–5} However, the substantial expense of these methods hinders their application to macromolecules with thousands of atoms. As a result of the increase of NMR studies of biological systems, empirical methods^{6–9} have been developed to reproduce measured chemical shifts by parametrization and have been shown to be useful in protein structure refinement.¹⁰ While they have been reasonably successful for protein systems, these empirical approaches are not designed to study protein–ligand complexes because a variety of ligand molecular structures generally are not in the parametrization set. Recently, we have developed a fast approach, DCNMR,¹¹ to calculate NMR chemical shifts using the divide-and-conquer method^{12–14} at the MNDO¹⁵ level.

* Corresponding author phone: (352) 392-6973; fax: (352) 392-8722; e-mail: merz@psu.edu.

[†] Current address: University of Florida, Department of Chemistry, Quantum Theory Project, 2328 New Physics Building, P. O. Box 118435, Gainesville, FL 32611. E-mail: merz@qtp.ufl.edu.

By utilizing parameters specifically developed for NMR calculation,¹⁶ excellent agreement with experimental results was obtained for ligand proton chemical shifts in the FK506 binding protein (FKBP)–GPI complex¹⁷ and cellular retinol-binding protein.¹⁸ Applications to decoy pose scoring¹⁷ and NMR structure refinement¹⁸ have been illustrated as well.

In this paper, we extend our DCNMR approach into the quantum mechanical/molecular mechanical (QM/MM) framework. The motivations for this work were as follows: (1) Although our original approach is able to compute NMR chemical shifts for macromolecules containing thousands of atoms, it is still computationally intensive to address these systems. Since the chemical shieldings are strongly dependent on local electronic environments, in many instances, it is unnecessary to treat all atoms in macromolecules by the more expensive quantum mechanical approach. (2) If the interest is localized in the binding site of the protein–ligand or protein–protein complex, it is natural to calculate NMR chemical shifts within the framework of QM/MM; the ligand and the residues inside the binding site are treated quantum mechanically, while the rest of system is computed molecular mechanically. (3) A good structure is a requirement for NMR chemical shift calculations. However, geometry optimization of an entire protein with several thousands of atoms is a substantial task even for linear-scaling semiempirical methods. If we can use QM/MM-optimized geometries for the NMR chemical shift calculation, it will significantly speed up the entire process.

A number of NMR chemical shift calculations using the QM/MM approach have been recently reported. Cui and Karplus¹⁹ have combined Gaussian and CHARMM to compute NMR chemical shifts using the QM/MM approach, and this is the most general implementation so far. Their results demonstrated that the QM/MM approach can reach the same accuracy as a full QM calculation by using hydrogen atoms as link atoms. By capping the QM region with quantum capping potentials and representing the MM region with point charges, Moon et al.²⁰ proposed a simple approach to calculate NMR shielding tensors since most quantum chemistry programs can handle effective core potentials and point charges. Another implementation of NMR chemical shift calculation using plane wave basis sets with repulsive potentials in conjunction with the QM/MM strategy has appeared as well.²¹ All these approaches utilized ab initio and DFT methods to treat the QM region, which might not be ideally suited for high-throughput screening studies of protein–ligand complexes, for example. The total number of atoms in the binding site (including the inhibitor and the residues around it) could be so large (potentially over 100 atoms) that the computational costs of current ab initio and DFT methods are still prohibitive for routine NMR chemical shift calculations. Moreover, it may be necessary to use a relatively large QM region to alleviate nonphysical effects arising from the use of link atom schemes at the boundary of the QM and MM regions. Here, we incorporate our fast DCNMR approach into AMBER to compute NMR chemical shifts using the QM/MM approach. This coupling makes it possible to provide insights into biomacromolecules using chemical shift information, such as building relation-

ships between predicted chemical shifts and the protein structure, studying dynamical effects on chemical shifts, and even performing virtual high-throughput NMR-based screening on large sets of molecules.

II. Method and Implementation

Since our DCNMR approach has been published elsewhere,¹¹ only the essentials relating to the QM/MM implementation are outlined herein. The chemical shielding tensor σ_{ab} is the second derivative of the molecular energy with respect to the external magnetic field and the nuclear magnetic moment, which can be expressed in the Hamiltonian form as

$$\sigma_{ab} = \sum_{\mu\nu} \mathbf{P}_{\mu\nu} H_{\mu\nu}^{ab} - \sum_{\mu\nu} \mathbf{P}_{\mu\nu}^a H_{\mu\nu}^{0b} \quad (1)$$

where $\mathbf{P}_{\mu\nu}$ is the density matrix obtained from the self-consistent field (SCF) calculation, $\mathbf{P}_{\mu\nu}^a$ is the derivative of the density matrix with respect to the magnetic field. $H_{\mu\nu}^{ab}$ and $H_{\mu\nu}^{0b}$ are the magnetic integral elements in the gauge-including atomic orbital. Their expressions are

$$H_{\mu\nu}^{0b} = -\frac{1}{c} \left\langle \chi_\mu \left| \frac{[(\vec{r} - \vec{R}) \times \vec{\nabla}]_b}{|\vec{r} - \vec{R}|^3} \right| \chi_\nu \right\rangle \quad (2)$$

$$H_{\mu\nu}^{ab} = \frac{1}{2c^2} \left\{ (\vec{R}_\mu \times \vec{R}_\nu)_a \left\langle \chi_\mu \left| \frac{[(\vec{r} - \vec{R}) \times \vec{\nabla}]_b}{|\vec{r} - \vec{R}|^3} \right| \chi_\nu \right\rangle + \left\langle \chi_\mu \left| \frac{[(\vec{r} - \vec{R}_\mu) \times (\vec{R}_\nu - \vec{R}_\mu)]_a}{|\vec{r} - \vec{R}|^3} \frac{[(\vec{r} - \vec{R}) \times \vec{\nabla}]_b}{|\vec{r} - \vec{R}|^3} \right| \chi_\nu \right\rangle + \left\langle \chi_\mu \left| \frac{\delta_{ab}(\vec{r} - \vec{R}_\nu)(\vec{r} - \vec{R}) - (\vec{r} - \vec{R}_\nu)_b(\vec{r} - \vec{R})_a}{|\vec{r} - \vec{R}|^3} \right| \chi_\nu \right\rangle \right\} \quad (3)$$

The detail implementation of these integrals was described in our original paper.¹¹ The perturbed density matrix $\mathbf{P}_{\mu\nu}^a$ can be obtained by solving the coupled-perturbed Hartree–Fock (CPHF) equations. However, current implementations of this procedure are time-consuming, although some efforts to reduce this cost have appeared.²² To take advantage of the linear-scaling divide-and-conquer method,^{12–14} we adopted an alternative approach to calculate the perturbed density matrix, which was based on finite perturbation theory. The magnetic-field-dependent Fock matrix was first built and diagonalized; then, the perturbed density matrix could be approximated by

$$\mathbf{P}_{\mu\nu}^a \approx \frac{iP_{\mu\nu}^i}{B_a} \quad (4)$$

where $P_{\mu\nu}^i$ is the imaginary part of the density matrix. Consequently, this approach enables us to calculate the density matrix and the perturbed density matrix simultaneously using the divide-and-conquer method.

The combination of quantum mechanics and molecular mechanics is a natural approach for the study of enzyme reactions and protein–ligand interactions.²³ The active site or binding site is treated by ab initio, density functional theory, or semiempirical potentials, whereas the rest of the

system is modeled via force fields. The corresponding Hamiltonian can be divided according to

$$\hat{H}_{\text{total}} = \hat{H}_{\text{QM}} + \hat{H}_{\text{MM}} + \hat{H}_{\text{QM/MM}} \quad (5)$$

In our approach, \hat{H}_{QM} can be MNDO,¹⁵ AM1,²⁴ and PM3²⁵ semiempirical methods implemented in the program DIVCON; \hat{H}_{MM} is determined by an AMBER force field. $\hat{H}_{\text{QM/MM}}$ describes the interaction between the QM and MM atoms. In general, it is written as

$$\hat{H}_{\text{QM/MM}} = -\sum_{iM} \frac{q_M}{r_{iM}} + \sum_{\alpha M} \frac{Z_{\alpha} q_M}{R_{\alpha M}} + \sum_{\alpha M} \left[\frac{A_{\alpha M}}{R_{\alpha M}^{12}} - \frac{B_{\alpha M}}{R_{\alpha M}^6} \right] \quad (6)$$

where the subscripts i and α refer to the QM electrons and nuclei, respectively, and M to the MM atoms. q_M is the MM partial charge. The first two terms are electrostatic terms through which the MM atoms interact with the QM electrons and nuclei, respectively. The last term is the van der Waals term.

As pointed out by Cui and Karplus,¹⁹ the MM atoms make contributions to the chemical shielding tensors through their perturbations on both the density matrix and the perturbed density matrix. In our DCNMR approach, both the density matrix and the perturbed density matrix are obtained simultaneously by the diagonalization of the complex Fock matrix without utilizing the more expensive CPHF equations. Therefore, it is straightforward to include the MM contributions to the chemical shielding tensors by simply adding the first term in eq 6 to the Fock matrix. The method described above has been implemented into a development version of DIVCON and AMBER8.²⁶

III. Results and Discussion

In this section, we apply the QM/MM DCNMR method to a number of model systems including the water dimer, crambin, and the FKBP–GPI complex. Our focus is on the validation of the QM/MM results with respect to the full QM calculations. Future work will focus on the application of this approach to biological problems.

III.1. Water Dimer. The water dimer is a simple hydrogen-bonded system for which chemical shielding changes associated with the variation of geometric parameters have been studied by full ab initio methods^{27,28} and the QM/MM method.¹⁹ To test our approach on the water dimer, a set of structures was generated by varying the distance between the two oxygen atoms. These structures were then optimized at the B3LYP/6-311++G** level. For each structure, the NMR chemical shifts of the hydrogen and oxygen atoms relative to the isolated water molecule were calculated as

$$\Delta\delta = \sigma_{\text{monomer}} - \sigma_{\text{dimer}} \quad (7)$$

In this way, the intrinsic errors associated with the methods will be largely canceled. In the QM/MM calculations, one water was treated by our MNDO/NMR approach and the other by the TIP3P model.²⁹ Comparisons of the chemical shifts between full QM and QM/MM methods are shown in Figure 1 for the donor, acceptor hydrogen atoms, and the

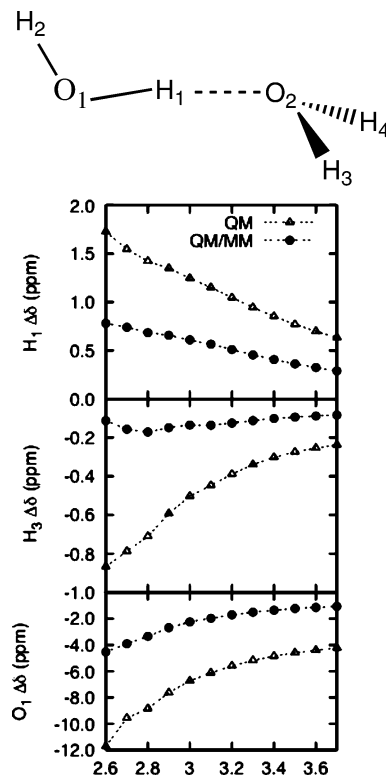


Figure 1. Comparison of the full QM and QM/MM chemical shifts for water dimers as a function of the hydrogen bonding O1...O2 distance (Å).

oxygen atom. Note that the energy minimum of the water dimer at the B3LYP/6-311++G** level occurs at 2.90 Å. The NMR chemical shifts for the donor hydrogen decrease monotonically as the internuclear distance increases, which is consistent with previous studies.^{19,27,28} However, the QM/MM curve decays much more slowly than the full QM one, and the chemical shift differences between the two curves are significant along the entire profile (as large as 0.7 ppm at the minimum energy distance). This discrepancy is due to the absence of the Pauli repulsion contribution in the QM/MM model. Similar trends are also shown for the acceptor hydrogen and the donor oxygen atom. This strongly suggests that hydrogen-bonded interactions have to be included as part of the QM region, which further confirms Cui and Karplus's conclusion.¹⁹

III.2. Crambin. Our second test system was crambin, a small hydrophobic protein with 46 residues. Both high-resolution X-ray and NMR structures are available for this protein. A small (cut 1) and a large (cut 2) QM/MM partitioning were tested for Ala9 and Pro5. As shown in Figure 2, cut 1 for Ala9 puts only the side-chain atoms in the QM region, and a link atom is introduced between the C α and C β bond, while in cut 2, the QM region is extended to the neighboring peptide bonds. Figure 3 demonstrates the partition scheme for Pro5. In cut 1, the QM region is Pro5 with the neighboring peptide bonds; cut 2 is cut 1 plus a nearby residue Tyr44. The MM part is treated with the AMBER parm94 force field.³⁰ The entire geometry was optimized at the AM1 level before the NMR shielding calculation. Full QM NMR calculations have also been carried out as reference values using our DCNMR approach.

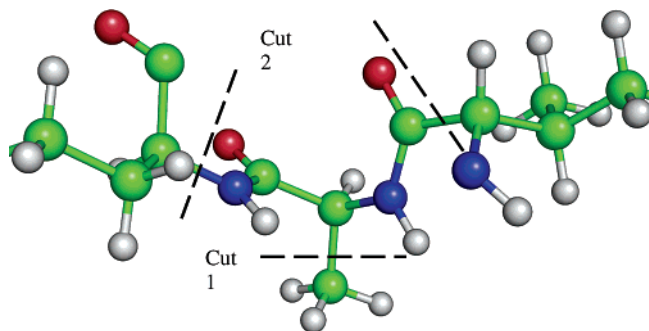


Figure 2. QM/MM partition scheme for Ala9 in crambin.

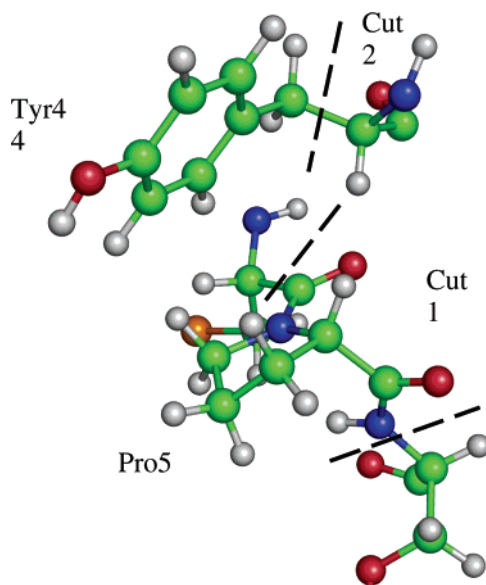


Figure 3. QM/MM partition scheme for Pro5 in crambin.

Table 1. Computed NMR Chemical Shift Errors (in ppm) at Different QM/MM Partition Schemes for Crambin Ala9 and Pro5

residue	atom	cut 1 ^a	cut 2
Ala9	CB	−22.25	0.791
	HB	−1.459	0.145
Pro5	CB	0.200	−0.373
	HB2	0.613	−0.238
	HB3	0.416	0.058
	CG	0.331	−0.270
	HG2	0.535	−0.240
	HG3	0.337	0.053
	CD	−0.251	−0.623
	HD2	0.146	−0.386
	HD3	0.233	0.046

^a Note that cut 1 and cut 2 are different for Ala9 and Pro5 (see text and Figures 2 and 3).

The differences between the QM/MM and full QM chemical shifts are summarized in Table 1. Obviously, the results for Ala9 using the cut 2 scheme are much better than that from cut 1; the error for the C β chemical shift is reduced from 22 to 0.7 ppm, and the errors for proton chemical shifts are also dramatically decreased from 1.5 to 0.15 ppm. This suggests that the peptide groups have significant magnetic susceptibilities and their effect on the chemical shieldings on the side-chain atoms is not negligible. Excellent agreement in

cut 2 also indicates that these interactions are generally short-ranged ($1/r^3$ according to the McConnell equation³¹). Therefore, we conclude that it is realistic to treat remote peptide bonds with MM. For Pro5, the inclusion of the peptide bond atoms was able to give comparable results for the carbon atoms but was not good enough to reproduce the full QM results for hydrogen atoms. The chemical shift errors for HB and HG are 0.6 and 0.4 ppm, respectively. This problem was alleviated through the addition of the proximal residue Tyr44 (cut 2 model) to the QM NMR calculation. This reduced the calculated errors to 0.05 and 0.03 ppm, respectively. These calculations have demonstrated that it is necessary to put nearby polar and aromatic rings into the QM region to obtain satisfactory results from the QM/MM NMR method.

III.3. FKBP-GPI Complex. NMR spectroscopy has become a useful tool to study protein–ligand interactions, an essential step for structure-based drug design. This is because protein–ligand complex structures can be solved by NMR, and many NMR-based screening techniques have been developed for lead discovery and optimization such as structure–activity relationships by NMR.³² The theoretically calculated chemical shieldings for a protein–ligand complex can aid in determining NMR structures and improve the accuracy of NMR screening techniques. We have carried out DCNMR calculations on the entire FKBP–GPI complex and obtained an excellent correlation between computed and experimental proton chemical shifts of the ligand.¹⁷ Figure 4 illustrates the GPI ligand and the binding site residues. To investigate the effect of QM/MM partitioning on chemical shift calculation, we tested three different partition schemes: The QM region for cut 1 was just the ligand itself, and the entire protein was treated using MM. In cut 2, the QM region extends to the side-chain atoms of all residues inside the binding pocket (including Tyr26, Phe36, Asp37, Phe46, Phe48, Gln53, Val55, Ile56, Trp59, Tyr82, His87, Ile90, Ile91, Leu97, and Phe99), which results in 275 QM atoms (excluding link atoms). Cut 3 was based on cut 2 and adds all backbone atoms for the binding site residues. The differences in proton chemical shifts between the QM/MM and full QM calculations are shown in Figure 5. It is not surprising that the results from cut 1 have relatively large deviations (RMSD: 1.12 ppm; RMSD = root-mean-square deviation) because it only includes ligand atoms in the QM region. Most of the errors arise from protons on the pyrrolidine ring, which is situated in the hydrophobic pocket formed by aromatic residues Tyr26, Phe46, Trp59, and Phe99. It demonstrates that the treatment of these residues as MM point charges cannot simulate realistic ring current effects. The inclusion of these aromatic residues into the QM region in cut 2 dramatically reduces the RMSD to 0.18 ppm. However, when we added backbone atoms into the QM region in cut 3, the agreement with the full QM results was slightly worse, with a RMSD of 0.28 ppm, which might be due to an imbalanced description at the QM and MM boundary.

The previous sets of NMR calculation were based on the AM1 optimized structure of the entire complex. Since the geometry optimization of the whole protein is a time-

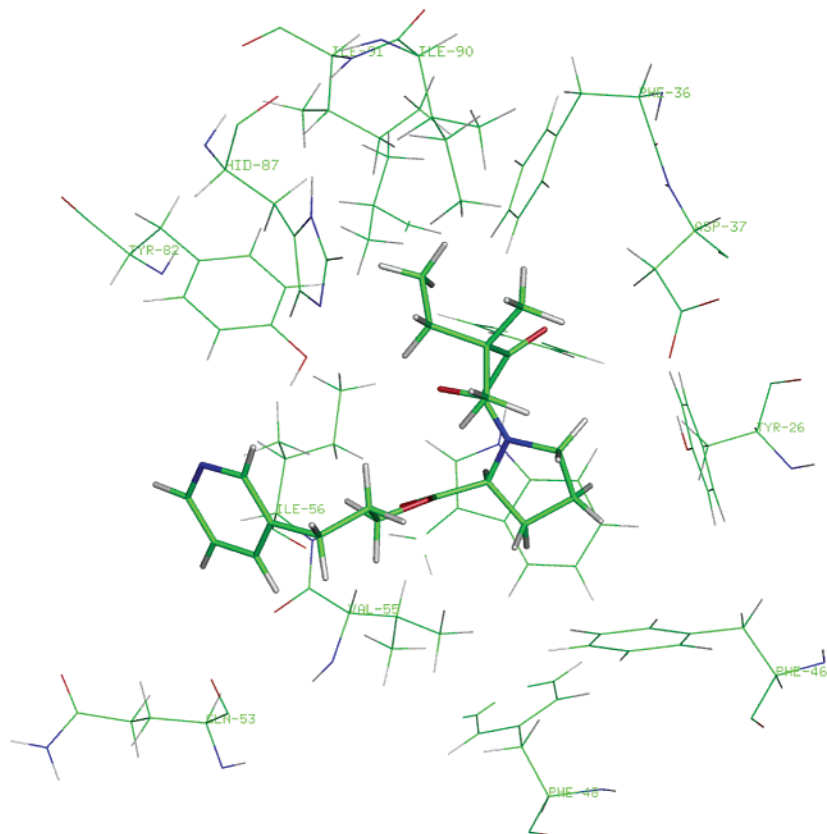


Figure 4. Binding site of FKBP–GPI complex.

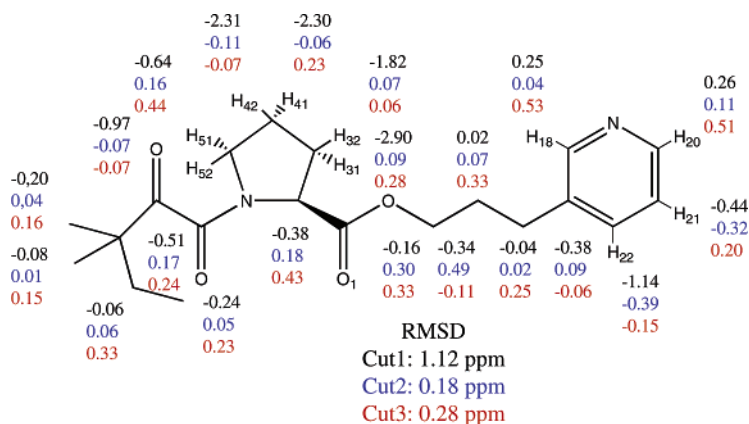


Figure 5. Chemical structure of the GPI molecule and the proton chemical shift errors for three different QM/MM partition schemes.

consuming step, another question we are trying to answer is whether we can use the less-expensive QM/MM-minimized structures for NMR calculation without compromising accuracy. Therefore, we carried out a 2000 step QM(AM1)/MM minimization of the FKBP–GPI complex based on the cut 2 scheme, followed by NMR calculation. The time saving is obvious since the total time of the QM/MM minimization was only about 2 days, while it took 8 days to optimize the entire complex by AM1 on our local opteron cluster, even with the divide-and-conquer approach. The all-atom RMSD of the binding site residues between the final geometry and full AM1 optimized geometry is only 0.7 Å. The RMSD of the calculated proton chemical shifts between the cut 2 scheme and the full QM result was 0.37 ppm. This agreement

indicates that the QM/MM-minimized structures are able to produce chemical shift results that are comparable to those from fully QM-optimized structures.

IV. Conclusions

We have coupled our recently developed DCNMR approach with AMBER to calculate NMR chemical shifts within the QM/MM framework. Because our approach is able to obtain both the density matrix and the perturbed density matrix in the SCF step, it is straightforward to include the MM contributions to our NMR chemical shift calculations. Application to the water dimer indicates that it is necessary to treat the whole hydrogen bond quantum mechanically. To

investigate the QM/MM partition effect on chemical shifts of a specific residue in a protein, we have carried out calculations on two residues of crambin using different QM/MM partitioning schemes. Good agreement with full QM results was obtained when the QM region included the nearby groups with significant magnetic susceptibilities such as peptide bonds and aromatic rings. Finally, the method was applied to a protein–ligand complex (FKBP–GPI), and the proton chemical shifts of the ligand were well reproduced when the side-chain atoms of the binding site residues were included in the QM region. We have also shown that the QM/MM-optimized structure is good enough to yield satisfactory results for NMR chemical shift calculations at a fraction of the cost of full QM geometry optimization. All these test calculations have demonstrated that our QM/MM NMR method with an appropriate QM/MM partition is able to obtain good agreement with full QM results at a much lower cost and, thus, paves a way to compute NMR chemical shifts for much larger macromolecules.

Acknowledgment. We thank the NSF (MCB-0211639) and the NIH (GM 44974) for support.

References

- (1) Wuthrich, K. *NMR of Proteins and Nucleic Acids*; Wiley: New York, 1986.
- (2) Spera, S.; Bax, A. Empirical Correlation between Protein Backbone Conformation and C-Alpha and C-Beta C-13 Nuclear-Magnetic-Resonance Chemical-Shifts. *J. Am. Chem. Soc.* **1991**, *113* (14), 5490–5492.
- (3) Rablen, P. R.; Pearlman, S. A.; Finkbiner, J. A comparison of density functional methods for the estimation of proton chemical shifts with chemical accuracy. *J. Phys. Chem. A* **1999**, *103* (36), 7357–7363.
- (4) Wang, B.; Fleischer, U.; Hinton, J. F.; Pulay, P. Accurate prediction of proton chemical shifts. I. Substituted aromatic hydrocarbons. *J. Comput. Chem.* **2001**, *22* (16), 1887–1895.
- (5) Wang, B.; Hinton, J. F.; Pulay, P. Accurate prediction of proton chemical shifts. II. Peptide analogues. *J. Comput. Chem.* **2002**, *23* (4), 492–497.
- (6) Osapay, K.; Case, D. A. A New Analysis of Proton Chemical-Shifts in Proteins. *J. Am. Chem. Soc.* **1991**, *113* (25), 9436–9444.
- (7) Williamson, M. P.; Kikuchi, J.; Asakura, T. Application of ¹H NMR chemical shifts to measure the quality of protein structures. *J. Mol. Biol.* **1995**, *247* (4), 541–546.
- (8) Wishart, D. S.; Watson, M. S.; Boyko, R. F.; Sykes, B. D. Automated ¹H and ¹³C chemical shift prediction using the BioMagResBank. *J. Biomol. NMR* **1997**, *10* (4), 329–336.
- (9) Xu, X. P.; Case, D. A. Automated prediction of ¹⁵N, ¹³C_{alpha}, ¹³C_{beta} and ¹³C' chemical shifts in proteins using a density functional database. *J. Biomol. NMR* **2001**, *21* (4), 321–333.
- (10) Osapay, K.; Theriault, Y.; Wright, P. E.; Case, D. A. Solution structure of carbonmonoxy myoglobin determined from nuclear magnetic resonance distance and chemical shift constraints. *J. Mol. Biol.* **1994**, *244* (2), 183–197.
- (11) Wang, B.; Brothers, E. N.; Van Der Vaart, A.; Merz, K. M. Fast semiempirical calculations for nuclear magnetic resonance chemical shifts: A divide-and-conquer approach. *J. Chem. Phys.* **2004**, *120* (24), 11392–11400.
- (12) Yang, W. T.; Lee, T. S. A Density-Matrix Divide-and-Conquer Approach for Electronic-Structure Calculations of Large Molecules. *J. Chem. Phys.* **1995**, *103* (13), 5674–5678.
- (13) Dixon, S. L.; Merz, K. M. Semiempirical molecular orbital calculations with linear system size scaling. *J. Chem. Phys.* **1996**, *104* (17), 6643–6649.
- (14) Dixon, S. L.; Merz, K. M. Fast, accurate semiempirical molecular orbital calculations for macromolecules. *J. Chem. Phys.* **1997**, *107* (3), 879–893.
- (15) Dewar, M. J. S.; Thiel, W. Ground State of Molecules. 38. The MNDO Method. Approximations and Parameters. *J. Am. Chem. Soc.* **1977**, *99* (15), 4899–4907.
- (16) Patchkovskii, S.; Thiel, W. NMR chemical shifts in MNDO approximation: Parameters and results for H, C, N, and O. *J. Comput. Chem.* **1999**, *20* (12), 1220–1245.
- (17) Wang, B.; Raha, K.; Merz, K. M., Jr. Pose scoring by NMR. *J. Am. Chem. Soc.* **2004**, *126* (37), 11430–11431.
- (18) Wang, B.; Merz, K. M., Jr. Validation of the binding site structure of the cellular retinol-binding protein (CRBP) by ligand NMR chemical shift perturbations. *J. Am. Chem. Soc.* **2005**, *127* (15), 5310–5311.
- (19) Cui, Q.; Karplus, M. Molecular properties from combined QM/MM methods. 2. Chemical shifts in large molecules. *J. Phys. Chem. B* **2000**, *104* (15), 3721–3743.
- (20) Moon, S.; Christiansen, P. A.; DiLabio, G. A. Quantum capping potentials with point charges: A simple QM/MM approach for the calculation of large-molecule NMR shielding tensors. *J. Chem. Phys.* **2004**, *120* (19), 9080–9086.
- (21) Sebastiani, D.; Rothlisberger, U. Nuclear magnetic resonance chemical shifts from hybrid DFT QM/MM calculations. *J. Phys. Chem. B* **2004**, *108* (9), 2807–2815.
- (22) Weber, V.; Niklasson, A. M. N.; Challacombe, M. *Phys. Rev. Lett.* **2004**, *92* (19), 193002.
- (23) Warshel, A.; Levitt, M. Theoretical studies of enzymic reactions: Dielectric, electrostatic and steric stabilization of the carbonium ion in the reaction of lysozyme. *J. Mol. Biol.* **1976**, *103*, 227–249.
- (24) Dewar, M. J. S.; Zoebisch, E. G.; Healy, E. F.; Stewart, J. J. P. AM1: A New General Purpose Quantum Mechanical Molecular Model. *J. Am. Chem. Soc.* **1985**, *107* (13), 3902–3909.
- (25) Stewart, J. J. P. Optimization of Parameters for Semiempirical Methods I. Method. *J. Comput. Chem.* **1989**, *10* (2), 209–220.
- (26) Case, D. A.; Darden, T. A.; Cheatham, I. T. E.; Simmerling, C. L.; Wang, J.; Duke, R. E.; Luo, R.; Merz, K. M.; Wang, B.; Pearlman, D. A.; Crowley, M.; Brozell, S.; Tsui, V.; Gohlke, H.; Mongan, J.; Hornak, V.; Cui, G.; Beroza, P.; Schafmeister, C.; Caldwell, J. W.; Ross, W. S.; Kollman, P. A. *AMBER*, 8.0; 2004.
- (27) Dithfield, R. Theoretical studies of magnetic shielding in H₂O and (H₂O)₂. *J. Chem. Phys.* **1976**, *65*, 3123–3133.

- (28) Chesnut, D. B.; Rusiloski, B. E. Partial energy and chemical shielding surfaces in the water (H₂O)₂ and hydrogen fluoride (HF)₂ van der Waals complexes. *J. Phys. Chem.* **1993**, 97, 2839–2845.
- (29) Jorgensen, W. L.; Chandrasekhar, J.; Madura, J. D.; Impey, R. W.; Klein, M. L. Comparison of simple potential functions for simulating liquid water. *J. Chem. Phys.* **1983**, 79, 926–935.
- (30) Cornell, W. D.; Cieplak, P.; Bayly, C. I.; Gould, I. R.; Merz, K. M., Jr.; Ferguson, D. C.; Spellmeyer, T.; Fox, J. W.; Caldwell, J. W.; Kollman, P. A. A Second Generation Force Field for the Simulation of Protein, Nucleic Acids, and Organic Molecules. *J. Am. Chem. Soc.* **1995**, 117, 5179–5197.
- (31) McConnell, H. M. Theory of Nuclear Magnetic Shielding in Molecules. I. Long-Range Dipolar Shielding of Protons. *J. Chem. Phys.* **1957**, 27, 226–229.
- (32) Shuker, S. B.; Hajduk, P. J.; Meadows, R. P.; Fesik, S. W. Discovering high-affinity ligands for proteins: SAR by NMR. *Science* **1996**, 274, 1531–1534.

CT050212S